

ORIGINAL ARTICLE

Threonine 209 phosphorylation on RUNX3 by Pak1 is a molecular switch for its dualistic functions

A Kumar^{1,7}, M Singhal^{1,7}, C Chopra^{1,7}, S Srinivasan¹, RP Surabhi¹, R Kanumuri¹, S Tentu¹, S Jagadeeshan¹, S Sundaram², K Ramanathan², R Shankar Pitani³, B Muthuswamy⁴, S Abhijit⁴, AS Nair⁵, G Venkatraman⁶ and SK Rayala¹

P21 Activated Kinase 1 (Pak1), an oncogenic serine/threonine kinase, is known to have a significant role in the regulation of cytoskeleton and cellular morphology. Runx3 was initially known for its role in tumor suppressor function, but recent studies have reported the oncogenic role of Runx3 in various cancers. However, the mechanism that controls the paradoxical functions of Runx3 still remains unclear. In this study, we show that Runx3 is a physiologically interacting substrate of Pak1. We identified the site of phosphorylation in Runx3 as Threonine 209 by mass spectrometry analysis and site-directed mutagenesis, and further confirmed the same with a site-specific antibody. Results from our functional studies showed that Threonine 209 phosphorylation in Runx3 alters its subcellular localization by protein mislocalization from the nucleus to the cytoplasm and subsequently converses its biological functions. This was further supported by *in vivo* tumor xenograft studies in nude mouse models which clearly demonstrated that PANC-28 cells transfected with the Runx3-T209E clone showed high tumorigenic potential as compared with other clones. Our results from clinical samples also suggest that Threonine 209 phosphorylation by Pak1 could be a potential therapeutic target and of great clinical relevance with implications for Runx3 inactivation in cancer cells where Runx3 is known to be oncogenic. The findings presented in this study provide evidence of Runx3-Threonine 209 phosphorylation as a molecular switch in dictating the tissue-specific dualistic functions of Runx3 for the first time.

Oncogene (2016) 35, 4857–4865; doi:10.1038/onc.2016.18; published online 22 February 2016

INTRODUCTION

Runt-related transcription factor 3 (Runx3) is a member protein belonging to the family of runt domain-containing transcription factors. Runx3 was initially known for its role in tumor suppression, but recent studies have revealed the paradoxical role of Runx3 in various cancer types.¹ It has been shown to have both tumor suppressor (pancreatic cancer, gastric cancer and esophageal cancer) and oncogenic effects (head and neck cancer, basal cell carcinoma and ovarian cancer).^{2–4} In addition to its localization in the nucleus, Runx3 is reported to be localized in the cytoplasm in various normal and cancer cell lines.⁵ Epigenetic inactivation *via* promoter hypermethylation,^{6,7} functional point mutations⁸ and protein mislocalization⁹ have been implicated in the mechanism of loss of tumor suppressor activity of Runx3. However, the mechanisms of mislocalization related to inactivation of Runx3 protein have not been deciphered fully. Post translational modifications, such as phosphorylation and acetylation, have long been accepted as important in the regulation of localization and function of Runx family.^{3,10} It has been shown that tyrosine phosphorylation of Runx3 by activated Src is associated with the cytoplasmic localization of Runx3 in gastric and breast cancers.¹¹ The prolyl isomerase Pin-1 has also been shown to inhibit the transcriptional activity of Runx3 by interacting with phosphorylated serine/threonine residues and inducing proteasome-mediated degradation.¹² Understanding the mechanism of this switch between a tumor suppressor and oncogenic function of

Runx3 is essential for having a better insight into the molecular mechanisms underlying tumor progression. In this study, we provide evidence that Runx3 is a physiologically interacting substrate of Pak1. This phosphorylation elucidates the mechanism of the intrinsic ability of Runx3 to shuttle between the nuclear and cytoplasmic compartments, which offers insight into the dual function of Runx3 in cancer.

RESULTS

Runx3 is a physiological substrate of Pak1

To determine whether Runx3 is a substrate of Pak1, we performed *in vitro* Pak1 kinase assay using GST-Runx3 as a substrate. Myelin basic protein, a well-known Pak1 substrate, was used as the positive control. The Pak1 enzyme efficiently phosphorylated GST-Runx3 as well as myelin basic protein (Figure 1a). There is no phosphorylation in the absence of Pak1 (Figure 1b). Further, to investigate whether Pak1 alone phosphorylates Runx3 or other PAKs of the subfamily (Pak2/Pak3) also phosphorylate Runx3, we performed *in vitro* kinase assay using GST-Runx3 as the substrate and their common substrate myelin basic protein as the experimental positive control. Results showed that Runx3 is exclusively a substrate of Pak1 and both Pak2 and Pak3 failed to phosphorylate Runx3 (Supplementary Figure 1). We next mapped the Pak1 phosphorylation domain in Runx3 using various deletion constructs of Runx3. GST fusion containing the

¹Department of Biotechnology, Indian Institute of Technology Madras (IITM), Chennai, India; ²Department of Pathology, Sri Ramachandra University, Chennai, India; ³Department of Community Medicine, Sri Ramachandra University, Chennai, India; ⁴Madras Diabetic Research Foundation (MDRF), Chennai, India; ⁵Rajiv Gandhi Centre for Biotechnology (RGCB), Thiruvananthapuram, India and ⁶Department of Human Genetics, Sri Ramachandra University, Chennai, India. Correspondence: Dr SK Rayala, Department of Biotechnology, Indian Institute of Technology Madras (IITM), Chennai 600036, India or Dr V Ganesh, Department of Human Genetics, Sri Ramachandra University, Chennai, India. E-mail: rayala@iitm.ac.in or ganeshv@sriramachandra.edu.in

⁷These authors contributed equally to this work.

Received 23 June 2015; revised 10 December 2015; accepted 18 December 2015; published online 22 February 2016

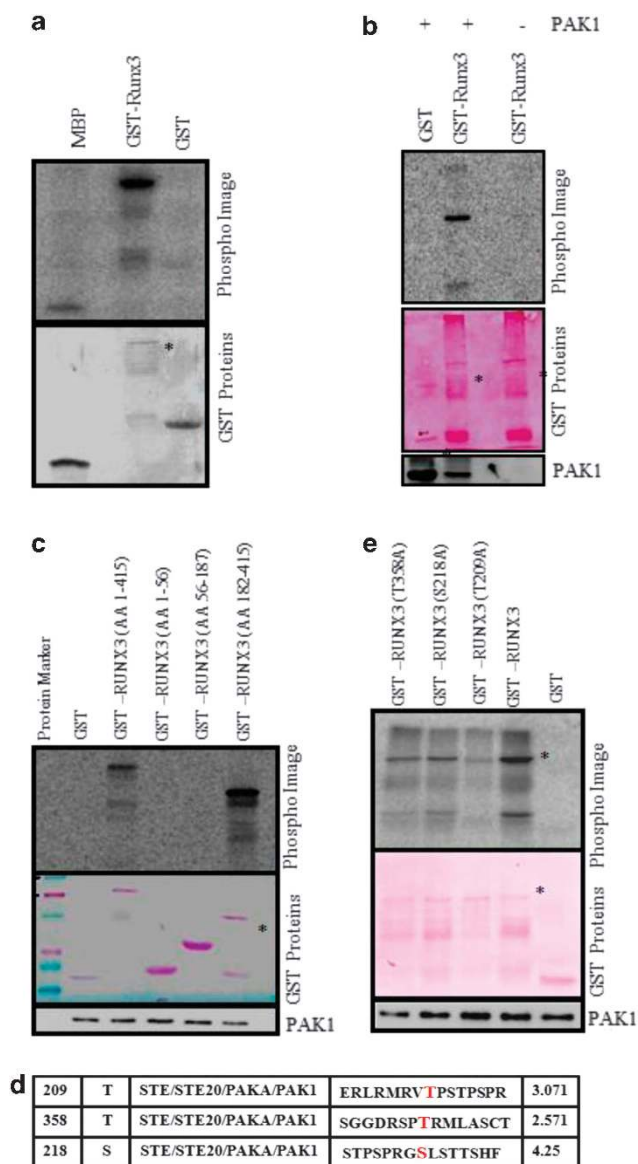


Figure 1. PAK1 phosphorylates Runx3 *in vitro* at Threonine 209 site. *In vitro* kinase assay with (a) GST, GST-Runx3 and myelin basic protein (positive control) as substrate and PAK1 as enzyme, (b) GST-Runx3 in presence or absence of PAK1 enzyme and (c) GST, GST-Runx3 (AA 1–415), GST-Runx3 (AA 1–57), GST-Runx3 (AA 56–187) and GST-Runx3 (AA 182–415) as substrate and PAK1 as enzyme. Pak1 was probed separately by western blotting. (d) Bioinformatic prediction of plausible PAK1 phosphorylation site in GST-Runx3 (AA 182–415) domain. (e) *In vitro* kinase assay with GST, GST-Runx3 (wt) and GST-Runx3 site-specific mutants—T209A, S218A and T358A—as substrate and PAK1 as enzyme. In all kinase assay images, GST protein represents ponceau-stained blot illustrating equal loading of proteins and phospho image represents autoradiogram image illustrating phosphorylated protein bands. Pak1 was probed separately by western blotting.

C-terminal of Runx3 alone was efficiently phosphorylated by Pak1 (Figure 1c, lane 6), suggesting the presence of a putative phosphorylation site in the C-terminal region. Analysis of the C-terminal amino acid sequence with group-based prediction tool (GPS) software revealed three plausible phosphorylation sites with high score for Pak1 phosphorylation (Figure 1d and the study by Kumar et al.¹³ for Pak1 phosphorylation consensus motif). To identify the exact site, we generated site-directed mutants

replacing the predicted Serine/Threonines (T209, S218 and T358) to Alanine in GST-Runx3 independently and performed the Pak1 kinase assay. Mutation of Threonine 209 on Runx3 to Alanine completely abolished the phosphorylation, indicating that T209 is the only site of Pak1 phosphorylation on Runx3 (Figure 1e). It was interesting to know that the T209 site is evolutionarily conserved across mammalian species (Supplementary Figure 2).

Further, to confirm the above findings in a cellular context, Cos-1 cells were transiently transfected with pcDNA vector, T7-tagged Runx3 and T7-tagged Runx3-T209A mutant, metabolically labeled with [³²P]orthophosphoric acid and T7-tagged proteins were immunoprecipitated with anti-T7 antibody agarose beads. As shown in Figure 2a, T7-tagged Runx3 showed significant amount of phosphorylation, whereas it was substantially blocked in the case of T7-tagged Runx3-T209A mutant. Next, we examined the change in RUNX3 phosphorylation with varying PAK1 activity using a physiological signal like EGF, and Sphingosine. Cos-1 cells transfected with T7-tagged Runx3 were metabolically labeled with [³²P]orthophosphoric acid and stimulated with EGF/Sphingosine, and T7-tagged Runx3 was immunoprecipitated with anti-T7 antibody agarose beads. The autoradiogram showed a substantial increase in the level of Runx3 phosphorylation in EGF- and Sphingosine-treated cells (Figure 2b). There was no effect of EGF on the phosphorylation of T7-tagged Runx3-T209A mutant (Supplementary Figure 3). Further, to examine the specific role of Pak1 in phosphorylation of Runx3, we used a siRNA specific to Pak1 to selectively deplete its expression. Introduction of Pak1 siRNA in Cos-1 cells transfected with T7-tagged Runx3 resulted in 50% reduction in the level of Pak1 protein and was accompanied by a 60% reduction in the Runx3 phosphorylation compared with its activity in control cells (Figure 2c, lane 3). To independently validate these findings, we repeated the experiment with Pak1 inhibitor IPA-3, a well-established inhibitor of Pak1 and its inactive analog PIR-3.5. As shown in Figure 2d, Runx3 phosphorylation was substantially blocked by Pak1 kinase inhibitor IPA-3, and there was no effect of PIR-3.5. Having established that Runx3 is phosphorylated in cellular context at Threonine 209, we next confirmed the Threonine 209 modification by mass spectrometry (Supplementary Figures 4 and 5).

Further, to directly demonstrate the Threonine 209 phosphorylation on Runx3 by Pak1, we performed *in vitro* Pak1 kinase assay using GST-Runx3 as a substrate and immunoblotted the membrane with pan anti-phosphothreonine antibody. Results showed that Runx3 is phosphorylated at threonine residue by Pak1 (Supplementary Figure 6). Furthermore, to directly demonstrate the existence of Threonine 209 phosphorylation on Runx3 under physiological conditions in a cellular context, we generated and characterized a site-specific antibody for Threonine 209 on Runx3 (Runx3-T209 phos). This Runx3-T209 phospho antibody recognizes only Runx3 phosphorylated on Threonine 209 *in vitro* and in cellular context. As evident from the blocking peptide assays, the antibody is very specific for phospho-Runx3 in immunohistochemistry (Figures 3a–e and Supplementary Figures 7–10). Collectively, these observations confirmed that Runx3 is a physiologic substrate of Pak1 and that T209 on Runx3 is the Pak1 phosphorylation site.

Runx3 interacts with Pak1 *in vitro* and in cellular context

Further, to test whether Runx3 interacts with Pak1, we evaluated the ability of *in vitro* translated Pak1 protein to bind with the Runx3-GST fusion protein. The Runx3-GST fusion protein, but not GST, efficiently interacted with ³⁵S-labeled full-length Pak1 protein (Figure 3f, left panel). Conversely, *in vitro* translated ³⁵S-labeled Runx3 protein specifically interacted with the GST-Pak1 (Figure 3f, right panel). In addition, we also performed surface plasmon resonance to show the interaction between Pak1 and Runx3 (Figure 3g). The cellular interaction of the endogenous Runx3 with

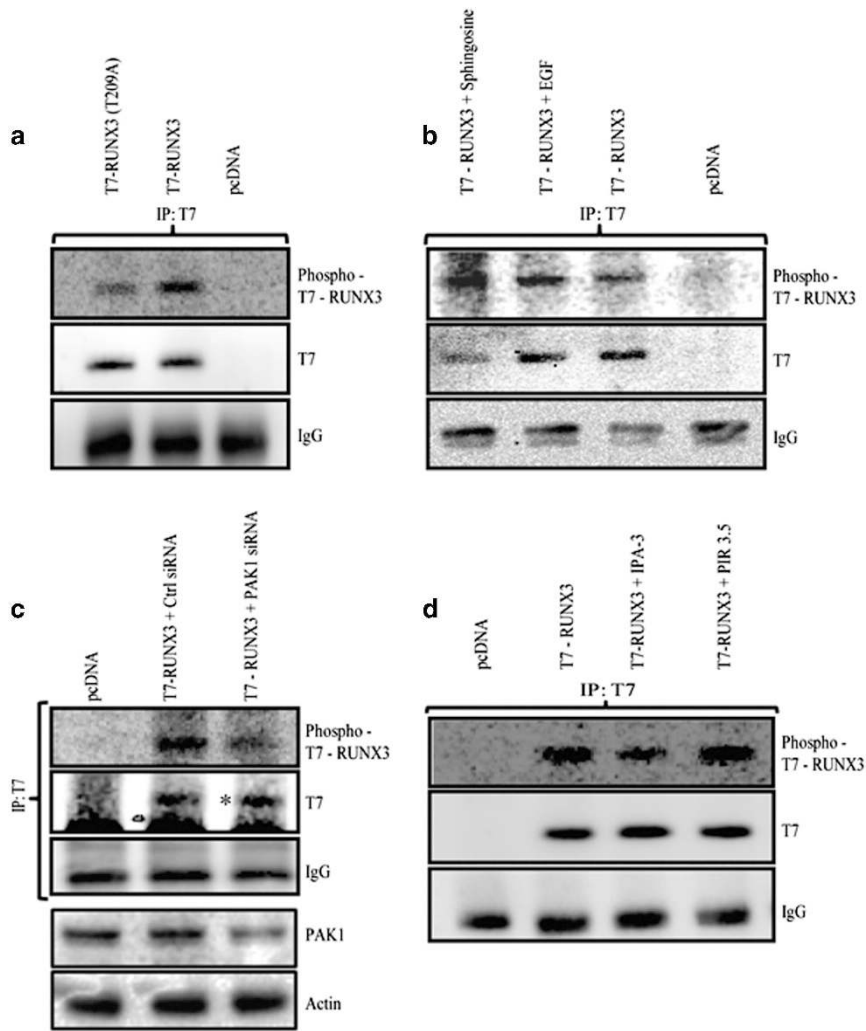


Figure 2. PAK1 phosphorylates RUNX3 in cellular context at Threonine 209. **(a)** Cos-1 cells were transfected with pcDNA, T7-RUNX3 (wt) or T7-RUNX3 (T209A) plasmids. After 24 h, transfected cells were metabolically labeled with p^{32} -orthophosphoric acid overnight, followed by T7 immunoprecipitation from cell lysates and gel electrophoresis. Phosphorylated protein bands were analyzed with autoradiogram images and subsequent immunoblotting with anti-T7 antibody. **(b)** Cos-1 cells were transfected with pcDNA or T7-RUNX3 (wt) plasmids. After 24 h, transfected cells were serum-starved and metabolically labeled with p^{32} -orthophosphoric acid overnight. Cells were then treated with EGF (100 ng/ml), Sphingosine (100 μ M) or 10% fetal bovine serum for 30 min, followed by T7 immunoprecipitation from cell lysates and gel electrophoresis. Phosphorylated protein bands were analyzed with autoradiogram images and subsequent immunoblotting with anti-T7 antibody. **(c)** Cos-1 cells were co-transfected with pcDNA or T7-RUNX3 (wt) plasmids and control or PAK1 siRNA. After 24 h, transfected cells were metabolically labeled with p^{32} -orthophosphoric acid overnight, followed by T7 immunoprecipitation from cell lysates and gel electrophoresis. Phosphorylated protein bands were analyzed with autoradiogram images and subsequent immunoblotting with anti-T7 antibody. PAK1 knockdown efficacy was determined by immunoblotting with anti-PAK1 antibody with actin as a house-keeping gene. **(d)** Cos-1 cells were transfected with pcDNA or T7-RUNX3 (wt) plasmids. After 24 h, transfected cells were serum-starved and metabolically labeled with p^{32} -orthophosphoric acid overnight. Cells were then treated with 20 μ M IPA-3 (PAK1 inhibitor) or 20 μ M PIR-3.5 (structural analog of IPA-3) for 30 min, followed by T7 immunoprecipitation from cell lysates and gel electrophoresis. Phosphorylated protein bands were analyzed with autoradiogram images and subsequent immunoblotting with anti-T7 antibody.

endogenous Pak1 was confirmed by immunoprecipitation of Pak1 and Runx3 using lysates from SCC-131 head and neck cancer cells and results showed that Pak1 interacted with Runx3 and vice versa (Figure 3h). In brief, these findings strongly suggested that Pak1 interacts with Runx3 in a physiologically relevant setting.

Modulating Pak1 levels alters the localization of Runx3

To further study the functional significance of Runx3-T209 phosphorylation, we generated stable Pak1 knockdown clones in head and neck squamous cell carcinoma cell line SCC-131, as this particular cell line has high levels of both Pak1 and Runx3 and will be an appropriate system to study functional changes due to changing phosphorylation levels of Runx3 upon Pak1 gene

silencing (Supplementary Figures 11A–C). As Runx3 is reported to have an oncogenic role in head and neck cancers and the hypothesis that ectopic localization of Runx3 from the nucleus to cytoplasm has been speculated to be associated with tumorigenesis prompted us to investigate the effect of Pak1 phosphorylation on subcellular localization of Runx3 in these Pak1 knockdown clones. Results showed that Runx3 is predominantly cytoplasmic in NT clones, whereas in Pak1 KD clones, it is relocated to the nuclear compartment (Figure 4a). The same is the case when treated with Pak1 siRNA or Pak1 inhibitor IPA-3 (Supplementary Figures 12 and 13). In support of this notion, nuclear and cytoplasmic protein fractions made from these clones also showed similar results (Figure 4b). To further confirm this, Cos-1 cells were transfected with pcDNA/Flag-Runx3/Flag-Runx3-

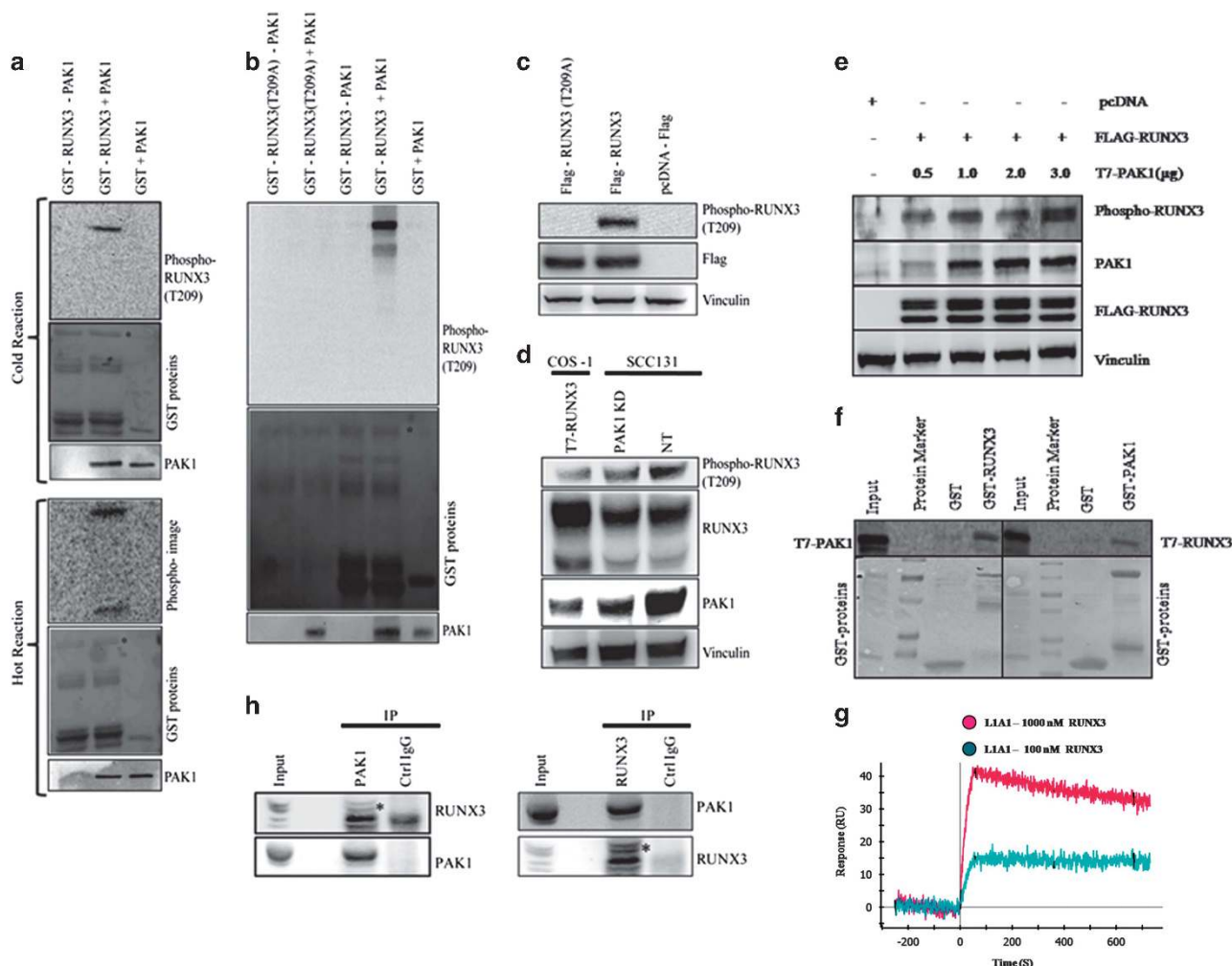


Figure 3. PAK1 physically interacts with RUNX3. **(a)** Characterization of anti-phospho-RUNX3 (T209) antibody using *in vitro* PAK1 kinase assay; comparing GST-Runx3 phosphorylation in the presence or absence of PAK1. Lower panel illustrates hot kinase assay (with P^{32} -labeled ATP) and upper panel includes parallel cold reaction immunoblotted with anti-phospho-Runx3 (T209) antibody. **(b)** *In vitro* kinase assay with GST, GST-Runx3 and GST-Runx3 (T209A) as substrate in the presence or absence PAK1 enzyme was performed. Proteins were immunoblotted with anti-phospho-Runx3 (T209) antibody. **(c)** Cos-1 cells were transfected with pcDNA-Flag, Flag-RUNX3 or Flag-RUNX3 (T209A). Total cell lysates were resolved on SDS-PAGE and immunoblotting is performed for anti-phospho-Runx3 (T209), anti-flag and anti-vinculin (house-keeping gene) antibodies. **(d)** Total cell lysates from SCC-131 stable PAK1 knockdown clone and non-target clone along with transient T7-Runx3-transfected Cos-1 cells (as positive control), were resolved by electrophoresis and immunoblotted for anti-phospho-Runx3 (T209), anti-Runx3, anti-PAK1 and anti-vinculin (house-keeping gene) antibodies. **(e)** Pak1 overexpression induces Runx3 phosphorylation at Threonine 209. Cos-1 cells were transfected with indicated concentration of Pak1 and immunoblotted for anti-phospho-Runx3 (T209). **(f)** GST pull-down assay was performed with GST-Runx3 as a bait and T7-PAK1 as a prey (Left panel) and GST-PAK1 as a bait and T7-Runx3 as a prey (right panel). **(g)** Representative sensorgram showing the binding of GST-Runx3 with the surface-immobilized PAK1. The red and blue curves represent the binding curves for 1000 nM and 100 nM concentrations of GST-Runx3, respectively. The surface immobilization of PAK1 was upto 3000 RUs. The KD value of 4.38×10^{-8} M was determined for Pak1-Runx3 interaction from the above two concentrations using Langmuir kinetic model. **(h)** Co-immunoprecipitation analysis was performed from SCC-131 total cell lysate by immunoprecipitating PAK1 and immunoblotting RUNX3 (left panel) and immunoprecipitating RUNX3 and immunoblotting PAK1 (right panel). In all kinase assay images, GST protein represents ponceau-stained blot illustrating equal loading of proteins and phospho image represents autoradiogram image illustrating phosphorylated protein bands.

T209A and Flag-Runx3-T209E constructs and localization of Runx3 was analyzed. Results showed that Flag-Runx3-T209E is localized to the cytoplasm, whereas the Flag-Runx3-T209A mutant is localized to the nucleus (Figure 5). Similar results were obtained when Cos-1 cells were transfected with pcDNA, Wt-Pak1 and Pak1-K299R (kinase dead Pak1) constructs (Supplementary Figure 14).

Runx3 loses its tumor suppressor activity upon phosphorylation by Pak1

The observed change in the localization of Runx3 by phosphorylation suggested that this mislocalization might have an influence on

the tumor suppressor activity of Runx3. To investigate the possibility, we measured the reporter activity of p21 promoter luciferase, which is known to be stimulated by Runx3. As shown in Figure 6a, Wt-Runx3 showed activation of p21 promoter as reported earlier,¹⁴ while Runx3-T209A mutant showed much higher activation of p21 promoter as compared with Wt-Runx3. This could be due to the significant nuclear localization of Runx3-T209A mutant, which was evident from the confocal imaging. The same was confirmed by analyzing p21 protein levels by western blotting (Figure 6b). These results were further confirmed by co-transfecting Pak1-T423E (kinase active) and Pak1-K299R (kinase dead) constructs along with Wt-Runx3 and

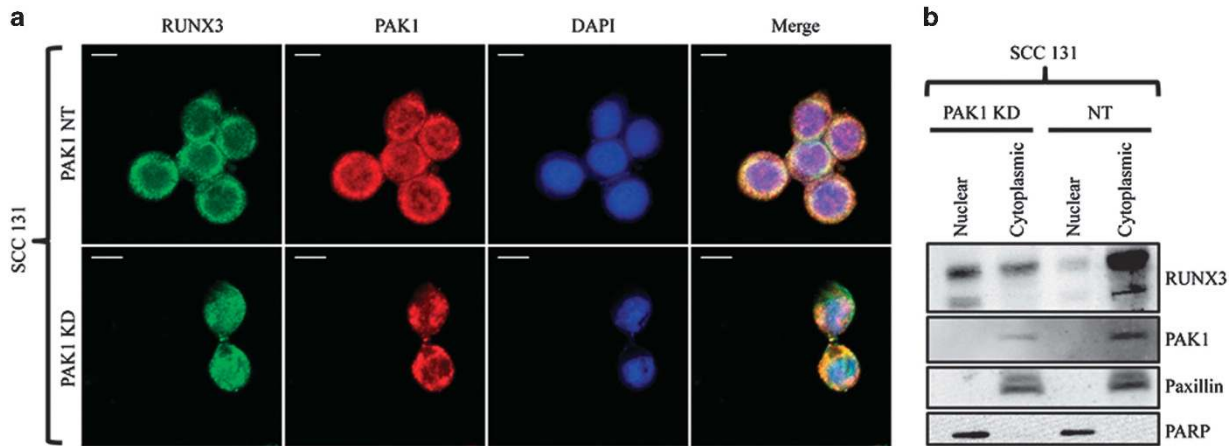


Figure 4. PAK1 phosphorylation sequesters RUNX3 in cytoplasmic compartment. **(a)** Immunofluorescence staining was performed on SCC-131 stable PAK1 knockdown and non-target control cells against RUNX3 (Alexa 488), PAK1 (Alexa 546) and DAPI (nuclear staining). **(b)** Subcellular fractions were isolated from SCC-131 stable PAK1 knockdown and non-target control cells, and separated using gel electrophoresis. Following the same, immunoblotting was performed with anti-RUNX3, anti-PAK1, anti-Paxillin (cytoplasmic marker) and anti-PARP (nuclear marker).

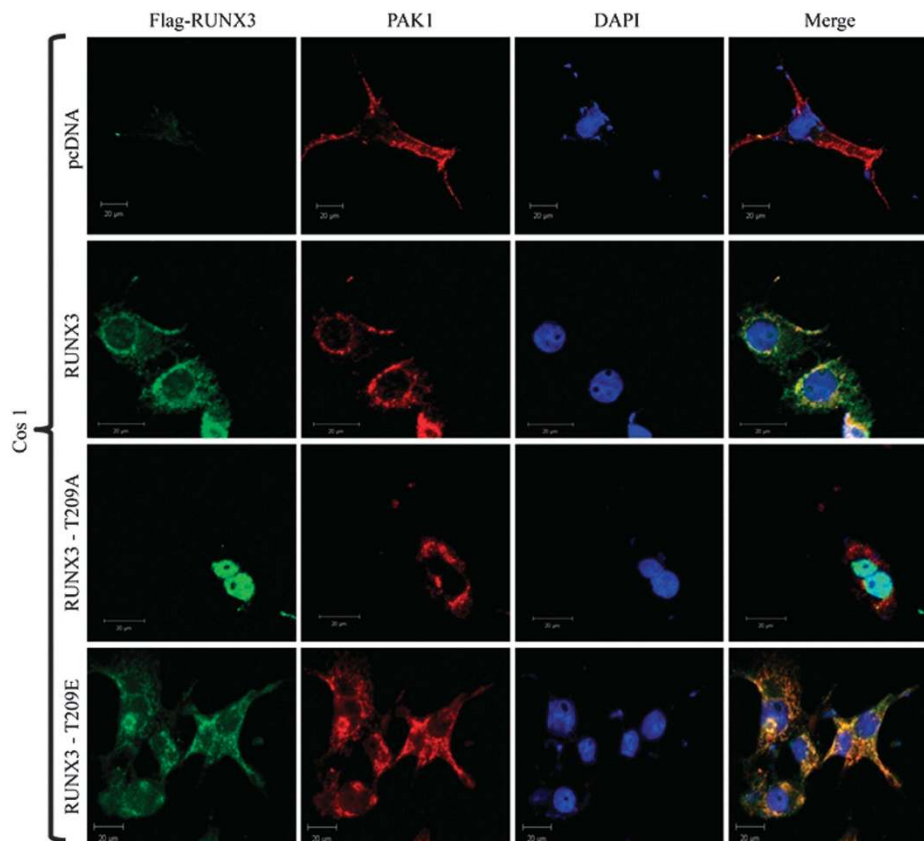


Figure 5. Differential localization of RUNX3 constructs. Cos-1 cells were transiently transfected with mammalian expression plasmid pcDNA-6A, tagged with FLAG. Cells were seeded on coverslips 24 h post transfection and cultured for another 24 h. Cells were probed using anti-FLAG antibody and anti-Pak1 antibody. Green coupled (Alexa 488) anti-mouse and red coupled (Alexa 546) anti-rabbit antibodies were used to visualize FLAG-tagged RUNX3 and PAK1, respectively. Wild-type cells showed predominant localization of RUNX3 in the cytoplasm, whereas T209A showed nuclear localization. T209E phospho-mimic cells showed cytoplasmic localization of RUNX3 similar to the wild type. All cells showed the presence of endogenous Pak1, indicating that the localization of Wt-RUNX3 is altered because of phosphorylation by Pak1.

results showed that co-expression of Pak1-T423E suppressed the Wt-Runx3-induced p21 promoter activity, whereas co-expression of Pak1-K299R had no effect on the p21 promoter activity induced by Wt-Runx3 (Figure 6c).

Oncogenic activity of T209-phosphorylated Runx3

To determine whether our findings were physiologically relevant in a system where Runx3 is reported to be a tumor suppressor, we established human pancreatic cancer cell lines stably

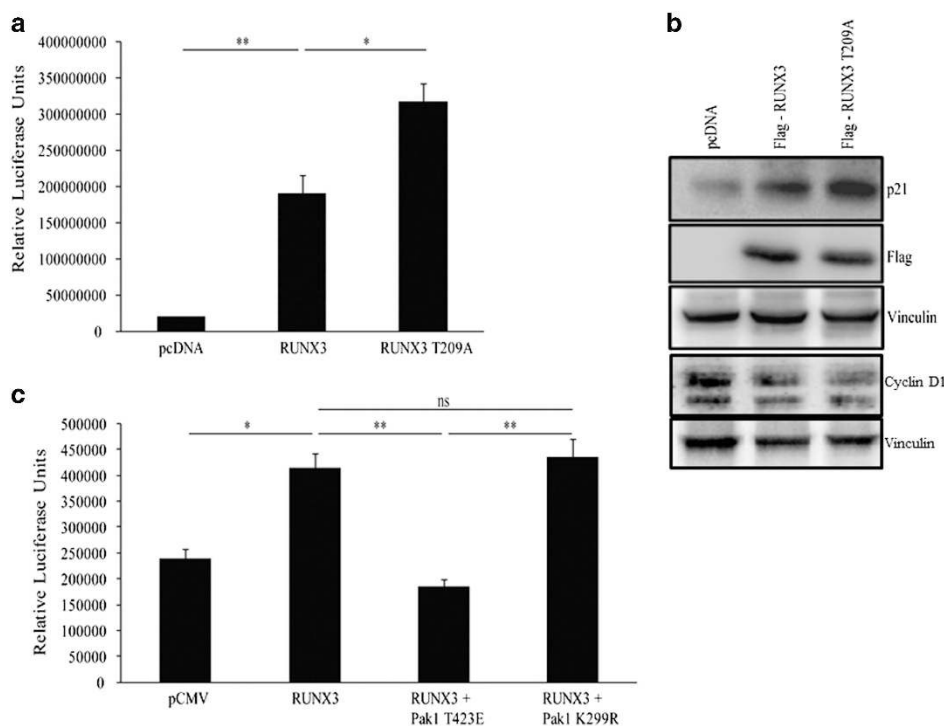


Figure 6. PAK1 phosphorylation switches off the tumor suppressor activity of RUNX3. **(a)** Cos-1 cells were co-transfected with p21^{CIP1/WAF1} promoter luciferase reporter construct and pcDNA or flag-RUNX3 (wt) or flag-RUNX3 (T209A) plasmid. After 24 h, cells were lysed; luciferase activity was measured ($n=3$) and normalized with respective β -galactosidase activity. Each value represents mean \pm s.e.m. $**P < 0.001$ and $*P < 0.05$, as compared with respective value. **(b)** Simultaneously, total cell lysates from **(a)** were separated using electrophoresis and were analyzed with immunoblotting using anti-p21, anti-flag, anti-Cyclin D1 and anti-vinculin (house-keeping) antibodies. Cyclin D1 and corresponding vinculin were run separately on another gel. **(c)** Cos-1 cells were co-transfected with p21^{CIP1/WAF1} promoter luciferase reporter construct and pCMV or flag-RUNX3 alone or flag-RUNX3 along with PAK1 (T423E) or flag-RUNX3 along with PAK1 (K299R). After 24 h, cells were lysed; luciferase activity was measured ($n=3$) and normalized with respective β -galactosidase activity. Each value represents mean \pm s.e.m. $**P < 0.0029$, $*P < 0.05$ and ns: non significant, as compared with respective value.

expressing pcDNA vector, Wt-Runx3, Runx3-T209E and Runx3-T209A in PANC28 cells and also verified their localization by confocal microscopy (Figure 7a and Supplementary Figure 15). As expected, stable clones overexpressing Wt-Runx3 and Runx3-T209A showed a decrease in the number of colonies formed in anchorage-independent soft agar and clonogenic cell survival assays as compared with vector control cells, whereas Runx3-T209E mutant showed an increase in the number of colonies in both these assays (Figures 7b and c), as compared with all other clones indicating that T209 phosphorylation on Runx3 contributes to the tumorigenic potential. In addition, stable clones overexpressing phosphorylation-active mutant Runx3-T209E showed high proliferation and enhanced wound-healing capability as compared with other clones, supporting the oncogenic activity of the phosphorylated Runx3 (Supplementary Figures 16A and B). This was further supported by *in vivo* tumor xenograft studies in nude mouse model which clearly demonstrated that PANC-28 stably transfected with Runx3-T209E clone showed high tumorigenic potential as compared with other clones. The mean tumor volume on day 10 itself for the Runx3-T209E clone was $74.8 \pm 17.14 \text{ mm}^3$ as compared with Runx3-T209A, which was only $37.92 \pm 11 \text{ mm}^3$ indicating the converse functional role of site-specific mutants (Table 1). After 4 weeks, the mean tumor volume of RUNX3-T209E clone was 128.12 ± 25.77 as compared with 85.08 ± 20.01 for pcDNA control indicating the role of phospho Runx3 as an oncogene (Figures 7d and e).

Further, to assess the relevance of our findings in cancer tissues and to characterize the efficiency of Runx3-T209 phospho antibody to detect phosphorylated Runx3 in paraffin-embedded tissues by immunohistochemistry (IHC), various human tissue array slides which had tumor cores along with adjacent normal

epithelium (matched) were used. We determined the expression of phospho-Runx3 on human tumor samples from four different anatomic sites, namely pancreatic ductal adenocarcinoma, head and neck squamous cell carcinomas, breast and ovarian carcinoma. The results of the immunohistochemistry staining clearly showed that the tumor samples had high expression of phospho-Runx3 as compared with the adjacent normal tissues. In breast, pancreatic and ovarian arrays, the phospho-Runx3 expression in the tumor tissues was predominantly localized in the cytoplasm, while some tissue sections showed faint focal nuclear positivity. There is a limitation that head and neck squamous cell carcinoma pathology results support our biochemistry localization findings only in a subset of cases. In the pancreatic ductal adenocarcinoma array, the mean Q score for the tumor samples was 10.16, as compared with the normal, which was only 6; similarly, head and neck squamous cell carcinoma samples had a mean Q score of 7.9, as compared with 6.09 for the adjacent normal mucosa. In the breast carcinoma array, the mean Q score for the tumor cores were 6.71 as compared with 3.6 in the adjacent normal breast epithelium. In the ovarian carcinoma tissue array, the mean Q score was 6 as compared with 2.5 in the normal ovarian epithelium from matched tissues. We applied paired *t* test, which showed good statistical significance. The data are represented in Table 2 and representative immunohistochemistry images are shown in Supplementary Figure 17. Furthermore, to evaluate the significance of our above findings, we examined the expression levels of phospho-Runx3 on human tumor samples from two different anatomic sites by western blotting. Results showed that phospho-Runx3 levels are significantly upregulated in tumor samples as compared with adjacent normal (Supplementary Figure 18).

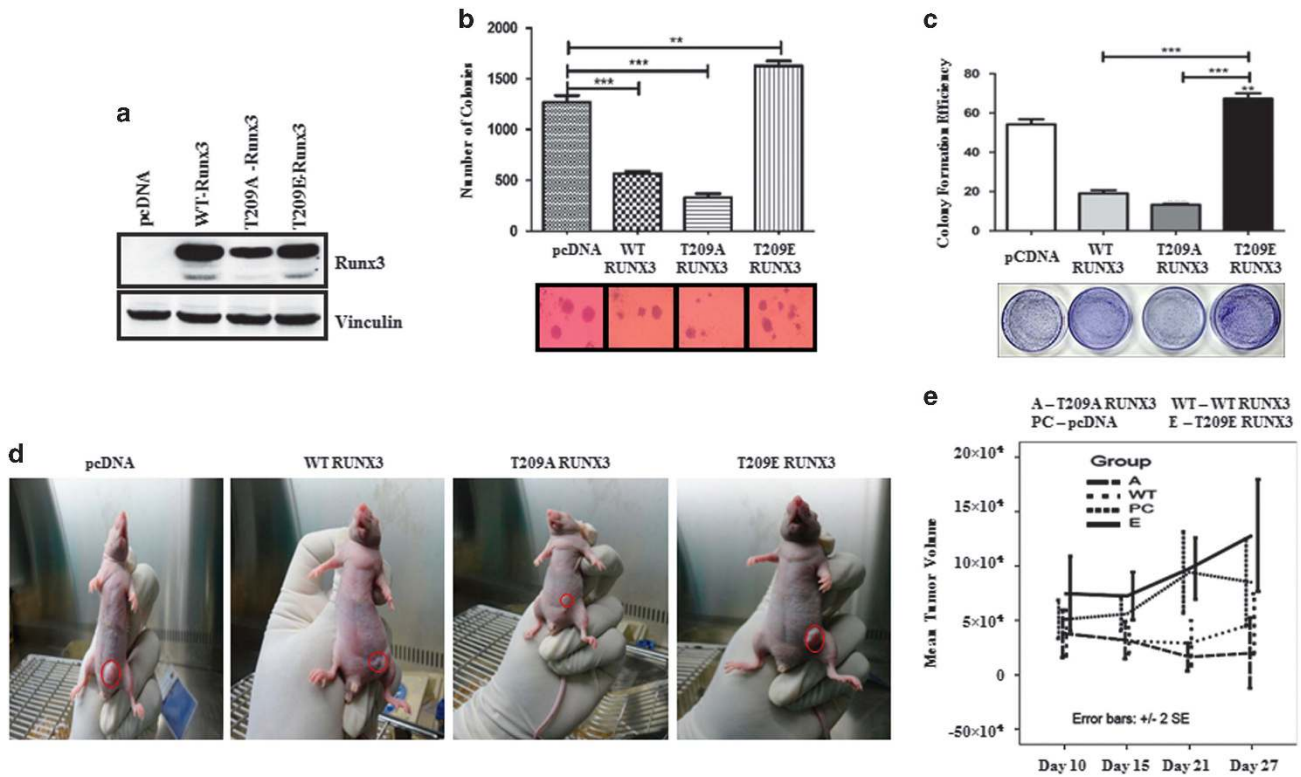


Figure 7. T209 phosphorylation on Runx3 by Pak1 is a switch regulating its dualistic functions. **(a)** Panc-28 stable overexpressing clones transfected with pcDNA, Wt-Runx3, Runx3-T209A and Runx3-T209E; 100 ug of total protein lysates were used for Runx3 probing. **(b and c)** Anchorage-independent soft agar and Clonogenic cell survival assay. Panc-28 cells stably overexpressing Wt-Runx3 and Runx3-T209A showed a significant decrease in the number of colonies formed in both the assays, whereas stably overexpressing Runx3-T209E Panc-28 cells showed a significant increase in the number of colonies when compared with vector control (pcDNA) cells. Each value represents the mean \pm s.e.m. *** $P < 0.001$, ** $P < 0.005$ compared with vector clones. **(d)** Representative tumor xenografts images of Panc-28 stable overexpressing clones of pcDNA, Wt-Runx3, Runx3-T209A and Runx3-T209E implanted subcutaneously in nude mice. **(e)** Graph showing tumor growth in nude mouse xenografts.

Table 1. Mean tumor volume of PANC-28 Runx3-transfected clones

	Mean tumor volume in mm ³ (s.e.m.) (n = 5)			
	PANC-28 A	PANC-28 wt	PANC-28 pcDNA	PANC-28E
Day 10	37.92 (11)	38.48 (10.58)	51.08 (8.8)	74.8 (17.14)
Day 15	32.06 (8.58)	31.49 (6.01)	56.10 (7.63)	72.56 (10.98)
Day 21	16.62 (6.45)	29.07 (10.42)	94.34 (74)	97.74 (14.14)
Day 27	20.11 (16.15)	46.94 (13.79)	85.08 (20.01)	128.12 (25.77)

Table 2. Q scores for pRUNX3 (Threonine 209) expression on human tumor tissue microarrays with adjacent normal

Tissue array	Samples (n)	Q scores (mean \pm s.d.)	P value
Pancreatic adenocarcinoma	25	Tumors: 10.16 \pm 2.7 Adjacent normal: 6.0 \pm 3.4	0.0005
Head and neck squamous cell carcinoma	22	Tumors: 7.9 \pm 3.3 Adjacent normal: 6.09 \pm 2.7	0.028
Breast carcinoma	21	Tumors: 6.71 \pm 4.91 Adjacent normal: 3.67 \pm 6.7	0.003
Ovarian carcinoma	16	Tumors: 6.0 \pm 4.53 Adjacent normal: 2.56 \pm 1.03	0.046

DISCUSSION

Protein phosphorylation is known to regulate protein nucleocytoplasmic localization in general and that Runx3 phosphorylation has been designated to lead to its cytoplasmic localization and thus loss of its tumor suppressor function. It was interesting to

note that Threonine 209 does not exist in Runx1 or Runx2 and therefore, it seems to have Runx3-specific function. This was further supported by the finding that among the group I Pak family, Pak1 alone (not Pak2 or Pak3) phosphorylates Runx3 and thereby Pak1 activity regulates its localization. Therefore, it is quite

possible that Pak1-being an oncogenic kinase-*per se* might be contributing to the tumorigenic potential *via* phosphorylating its substrate Runx3. In contrary to the reports on the tumor-suppressive role of RUNX3, several recent studies showed that RUNX3 can also function as an oncogene in certain types of cancers.^{2,3,15,16} Very recently, it was shown that Runx3 functions as both tumor suppressor and tumor promoter in pancreatic ductal adenocarcinoma by regulating the balance between proliferation and dissemination of pancreatic cancer cells in response to gene dosage of DPC4.¹⁷ Tsunematsu *et al.*¹⁸ reported that Runx3 has an oncogenic role in head and neck cancers that could be due to promoter demethylation during cancer development. They reported that Runx3 is localized to the nucleus. However, this nuclear localization is nowhere related or linked to the oncogenic activity of Runx3. In addition, the localization change will be in response to a signal and also depends on the percentage of Runx3 that is present in nucleus and cytoplasm at basal level in that particular tissue type. In addition, the regulation and diversifying role of Runx3 might also depend on its interacting proteins.¹⁹ In this study, we identified a single phosphorylation modification on Runx3 as a molecular switch that alters its subcellular localization and function, which in turn dictates the cell fate. This implies that the change in localization correlates to the levels of Pak1 activity in that particular tissue or cell line. Further, the existence of Runx3-Threonine 209 phosphorylation on a significant number of human tumor samples from different anatomic sites indicates that this is a common regulatory pathway that exists in different tissue types. In view of this, it would be worthwhile to explore this phosphorylation modification on Runx3 as a novel biomarker and as a potential therapeutic target in subset of cancer patients where Runx3 is overexpressed. In conclusion, we demonstrate PAK1-mediated Runx3 posttranslational modification acts as a functional rheostat in multiple cancer types, and it is also important to be cautious that this whole mechanism is not applicable if Runx3 is silenced by either hypermethylation or chromosomal aberration.

EXPERIMENTAL PROCEDURES

Cell culture and maintenance

All the cell lines were maintained in RPMI-1640/DMEM, unless otherwise specified. Additional details are provided in Supplementary data.

Plasmid constructs and bacterial strains

GST-tagged Runx3 (pGEX-4T1) full-length and deletion constructs were gifted by Prof Y Ito, Cancer Science Institute, NUS, Singapore. p21 (CIP1/WAF1)-Luciferase, pGL3-Basic, pcDNA 3.1-Flag and pcDNA 3.1-Flag-RUNX3 were gifted by Prof S ChulBae, Chungbuk National University, South Korea. T7-PAK1 (wild type), active PAK1 (T423E) and kinase dead PAK1 (K299R) constructs were purchased from Addgene (Cambridge, MA, USA). Additional details are provided in Supplementary data.

Antibodies, reagents and chemicals

The following antibodies were used: Runx3 (R3-5G4, Santa Cruz Biotechnology, Dallas, TX, USA), PAK1 (Cell Signaling Technology, Beverly, MA, USA), Vinculin (Sigma Aldrich, St Louis, MO, USA), β -Actin (Sigma Aldrich), T7 (Bethyl labs, Montgomery, TX, USA), GST (Millipore, Darmstadt, Germany), 6xHis (Millipore), Anti-PARP and anti-paxillin antibodies (Cell Signaling Technology) and anti-phosphothreonine (Millipore). Anti-phosphoRUNX3 (T209) rabbit polyclonal antibody was generated by Bioklone Private Limited (Bioklone, Chennai, India). Additional details are provided in Supplementary data.

In vitro kinase assay

GST-tagged RUNX3 wild-type and mutant proteins were used for *in vitro* kinase assays with GST as control. Forty microliters of the purified protein were taken and 10 μ l of ice cold 5 \times PAK1 kinase buffer were added to it.

The assays were carried out using radioactive γ P³²-ATP, in the presence or absence of PAK1 and the samples were incubated at 30 °C for 30 min.

In vivo metabolic labeling

Cells were seeded in 60 mm dishes and transfected with pcDNA or T7-RUNX3 (wild-type and mutant constructs as indicated) plasmids. After 24 h, the cells were labeled with P³²-orthophosphate in phosphate-free DMEM supplemented with pyruvate.

Surface plasmon resonance

The surface plasma resonance experiment was performed with Proteon XPR36 protein interaction array system (Bio-Rad, Hercules, CA, USA) at 25 °C using a GLC amine coupling proteon sensor chip. Additional details are provided in Supplementary data.

Mass spectrometry

The samples were digested with trypsin (Sequencing grade, Promega, Madison, WI, USA) and the digested peptides were analyzed on LTQ-Orbitrap Velos Elite (Thermo Electron, Bremen, Germany) coupled with easy nLC system (Thermo Scientific, Bremen, Germany). Additional details are provided in Supplementary data.

Immunohistochemistry

Human tissue microarrays with corresponding normal tissues were purchased from ISU ABXIS AccuMax (San Diego, CA, USA) or PANTOMICS (Richmond, CA, USA). Polyclonal anti-human phosphor Runx3 (T209) primary antibody was used and slides were scored by pathologist. Additional details are provided in Supplementary data.

Animal studies

Six-week-old *nu/nu* mice were purchased from Vivo Biotech, Hyderabad, India, after obtaining ethical clearance. Mice were divided into four groups ($n=5$) and injected subcutaneously using a 25-gauge needle with 10×10^6 PANC-28 stable overexpression clones of pcDNA/Runx3-Wt/Runx3-T209A or Runx3-T209E cells. The growth of xenografts was monitored. The statistical analysis of the data was carried out using the SPSS software Version 16.

Statistical analysis

Data are expressed as the mean \pm s.e.m. and analyzed by Student's *t*-test using Sigma Plot (SYSTAT software Inc., Chicago, IL, USA). *P* value < 0.05 is considered significant.

CONFLICT OF INTEREST

The authors declare no conflict of interest.

ACKNOWLEDGEMENTS

We thank Prof Yoshiaki Ito, Cancer Science Institute of Singapore, Singapore, for providing us the Runx3 constructs. We profusely thank Prof Susanne M Gollin, University of Pittsburgh, for providing us with SCC-131 cells. We thank Dr Marsha Fraizer (University of Texas, M. D. Anderson Cancer Center, USA); for providing MDA Panc 28 cells. We thank Dr Rajeshwari, Bioklone, Chennai, for generating polyclonal Runx3-Threonine 209 phospho antibody. We thank DAE-BRNS (Grant # 35/14/41/2014-BRNS-RTAC), DBT (BT/PR14340/NNT/28/860/2015) Government of India for financial support to SKR and the Department of Biotechnology, Indian Institute of Technology Madras (IITM) for infrastructural facilities. We thank Mr Balabhaskara Rao and Ms Lakshmi Arivazhagan for the initial help with protein expression studies and Runx3 clones. We thank Professor SP Thyagarajan, Dean Research and Management of SRU for Support and encouragement.

AUTHOR CONTRIBUTIONS

AKC, MS, CC, SSS, RS, ST, RK and SJ – performed experiments; SS and KR – stained and scored the IHC slides; SA and DB – helped with immunofluorescence studies; RSP – performed statistical analysis; ASN – helped with clinical samples; GV, MS and SKR – designed the study and experiments and wrote the paper.

REFERENCES

- 1 Chuang LS, Ito K, Ito Y. RUNX family: Regulation and diversification of roles through interacting proteins. *Int J Cancer* 2013; **132**: 1260–1271.
- 2 Kudo Y, Tsunematsu T, Takata T. Oncogenic role of RUNX3 in head and neck cancer. *J Cell Biochem* 2011; **112**: 387–393.
- 3 Chuang LS, Ito Y. RUNX3 is multifunctional in carcinogenesis of multiple solid tumors. *Oncogene* 2010; **29**: 2605–2615.
- 4 Bae SC, Choi JK. Tumor suppressor activity of RUNX3. *Oncogene* 2004; **23**: 4336–4340.
- 5 Ito K, Liu Q, Salto-Tellez M, Yano T, Tada K, Ida H *et al*. RUNX3, A novel tumor suppressor, is frequently inactivated in gastric cancer by protein mislocalization. *Cancer Res* 2005; **65**: 7743–7750.
- 6 Li QL, Ito K, Sakakura C, Fukamachi H, Ki I, Chi XZ *et al*. Causal relationship between the loss of *RUNX3* expression and gastric cancer. *Cell* 2002; **109**: 113–124.
- 7 Yanagawa N, Tamura G, Oizumi H, Takahashi N, Shimazaki Y, Motoyama T. Promoter hypermethylation of tumor suppressor and tumor-related genes in non-small cell lung cancers. *Cancer Sci* 2003; **94**: 589–592.
- 8 Kim WJ, Kim EJ, Jeong P, Quan C, Kim J, Li QL *et al*. RUNX3 inactivation by point mutations and aberrant DNA methylation in bladder tumors. *Cancer Res* 2005; **65**: 9347–9354.
- 9 Lau QC, Raja E, Salto-Tellez M, Liu Q, Ito K, Inoue M *et al*. RUNX3 is frequently inactivated by dual mechanisms of protein mislocalization and promoter hypermethylation in breast cancer. *Cancer Res* 2006; **66**: 6512–6520.
- 10 Bae SC, Lee YH. Phosphorylation, acetylation and ubiquitination: the molecular basis of RUNX regulation. *Gene* 2006; **366**: 58–66.
- 11 Goh YM, Cinghu S, Hong ET, Lee YS, Kim JH, Jang JW *et al*. Src kinase phosphorylates RUNX3 at tyrosine residues and localizes the protein in the cytoplasm. *J Biol Chem* 2010; **285**: 10122–10129.
- 12 Nicole Tsang YH, Wu XW, Lim JS, Wee Ong C, Salto-Tellez M, Ito K *et al*. Prolyl isomerase Pin1 downregulates tumor suppressor RUNX3 in breast cancer. *Oncogene* 2012; **32**: 1488–1496.
- 13 Kumar R, Gururaj AE, Barnes CJ. p21-activated kinases in cancer. *Nat Rev Cancer* 2006; **6**: 459–471.
- 14 Chi XZ, Yang JO, Lee KY, Ito K, Sakakura C, Li QL *et al*. RUNX3 suppresses gastric epithelial cell growth by inducing *p21^{WAF1/Cip1}* expression in cooperation with transforming growth factor β -activated SMAD. *Mol Cell Biol* 2005; **25**: 8097–8107.
- 15 Lee CW, Chuang LS, Kimura S, Lai SK, Ong CW, Yan B *et al*. RUNX3 functions as an oncogene in ovarian cancer. *Gynecol Oncol* 2011; **122**: 410–417.
- 16 Yoshiaki Ito. Oncogenic potential of the RUNX gene family: 'Overview'. *Oncogene* 2004; **23**: 4198–4208.
- 17 Martin CW, Kamel I, Rani PG, Libing F, Markus AC, Kathleen ED *et al*. RUNX3 controls a metastatic switch in pancreatic ductal adenocarcinoma. *Cell* 2015; **161**: 1–16.
- 18 Tsunematsu T, Kudo Y, Iizuka S, Ogawa I, Fujita T, Kurihara H *et al*. Runx3 has an oncogenic role in Head and Neck Cancer. *PLoS One* 2009; **4**: e5892.
- 19 Chauang LS, Ito K, Ito Y. RUNX family: Regulation and diversification of roles through interacting proteins. *Int J Cancer* 2013; **115**: 1260–1271.

Supplementary Information accompanies this paper on the Oncogene website (<http://www.nature.com/onc>)